DOI:
10.1177/0309133319841300

Document Version
Peer reviewed version

Progress in
Physical Geography

Estimating habitat extent and carbon loss from an eroded Northern blanket bog using UAV derived imagery and topography.

Journal:	*Progress in Physical Geography*
Manuscript ID	PPG-17-088.R3
Manuscript Type:	Main Article
Keywords:	Peatlands, Unmanned Aerial Vehicle, Structure from Motion, Habitat, Blanket Bog, Random Forest
Abstract:	Peatlands are important reserves of terrestrial carbon and biodiversity, and given that many peatlands across the UK and Europe exist in a degraded state, their conservation is a major area of concern, and a focus of considerable research. Aerial surveys are valuable tools for habitat mapping and conservation and provide useful insights into their condition. We investigate how Structure from Motion (SfM) photogrammetry derived topography and habitat classes may be used to derive an estimate of carbon loss from erosion features in a remote blanket bog habitat. An autonomous, unmanned, aerial, fixed wing remote sensing platform (Quest UAV 300™), collected imagery over Moor House – Upper Teesdale National Nature Reserve, a site with a high degree of peatland erosion. The images were used to generate point clouds into orthomosaics and digital surface models using SfM photogrammetry techniques, georeferenced, and subsequently used to classify vegetation and peatland features. A classification of peatbog feature types was developed using a random forest classification model trained on field survey data and applied to UAV-captured products including the orthomosaic, digital surface model and derived surfaces such as topographic index, slope and aspect maps. Using the area classified as eroded peat, and the derived digital surface model, we estimated a loss of 438 tonnes of carbon from a single gully. The UAV system was relatively straightforward to deploy in such a remote and unimproved area. SfM photogrammetry, imagery and random forest modelling obtained classification accuracies of between 42% and 100%, and was able to discern between bare peat, saturated bog and sphagnum, habitats. This paper shows what can be achieved with a low-cost UAV equipped with consumer grade camera equipment, and relatively straightforward ground control, and demonstrates their potential for the carbon and peatland conservation research community.

Abstract

Peatlands are important reserves of terrestrial carbon and biodiversity, and given that many peatlands across the UK and Europe exist in a degraded state, their conservation is a major area of concern, and a focus of considerable research. Aerial surveys are valuable tools for habitat mapping and conservation and provide useful insights into their condition. We investigate how Structure from Motion (SfM) photogrammetry derived topography and habitat classes may be used to derive an estimate of carbon loss from erosion features in a remote blanket bog habitat. An autonomous, unmanned, aerial, fixed wing remote sensing platform (Quest UAV 300™), collected imagery over Moor House – Upper Teesdale National Nature Reserve, a site with a high degree of peatland erosion. The images were used to generate point clouds into orthomosaics and digital surface models using SfM photogrammetry techniques, georeferenced, and subsequently used to classify vegetation and peatland features. A classification of peatbog feature types was developed using a random forest classification model trained on field survey data and applied to UAV-captured products including the orthomosaic, digital surface model and derived surfaces such as topographic index, slope and aspect maps. Using the area classified as eroded peat, and the derived digital surface model, we estimated a loss of 438 tonnes of carbon from a single gully. The UAV system was relatively straightforward to deploy in such a remote and unimproved area. SfM photogrammetry, imagery and random forest modelling obtained classification accuracies of between 42% and 100%, and was able to discern between bare peat, saturated bog and sphagnum, habitats. This paper shows what can be achieved with a low-cost UAV equipped with consumer grade camera equipment, and relatively straightforward ground control, and demonstrates their potential for the carbon and peatland conservation research community.

Introduction

Blanket bogs are tree-less habitats that form in cool, wet, oceanic climates dominated by vascular plants such as *Eriophorum* and *Calluna* spp and cushion forming bryophytes such as *Sphagnum* spp. They cover roughly 4,000,000 km^2 land and have been estimated to store 500-600 gigatonnes of carbon (Yu, 2012, Holden, 2005). Because of this enormous carbon (C) stock, peatland C represents an important reservoir within the global C cycle (Freeman et al. 2001). Over 80% of UK peatlands are in a degraded state due mainly to past drainage, fire and grazing (Joosten et al., 2012). It has been estimated that 16% of the global peatland reserve has been degraded and lost owing to human activities (Littlewood, 2010). Recently, the increased awareness of this global decline has resulted in a range of directives and guidelines, and in the UK conservation management aimed at restoring peatlands has been implemented under the EU habitats directive (Evans et al. 2014). From an ecological perspective, peatlands also represent an important habitat for a number of rare and endangered plant and animal species.

The monitoring of blanket bogs is particularly challenging, as a consequence of their remoteness and physical complexity, but a number of methods have been developed (Mc Morrow et al., 2004, Evans and Lindsay, 2010, Glendell et al., 2017). Remote sensing techniques using commercial satellite data are well established, and offer data at sub-10 m resolution. To date the high cost of these data, and limitations due to cloud coverage or view angles, have limited the value of Earth Observation (EO)-based data for this type of surveillance. Recently however, new methods for capturing high resolution scenes of remote peatlands have emerged.

Unmanned aerial vehicles (UAVs) now offer the ecologist a useful platform for capturing images of peatlands closer to the ground, i.e. below normal cloud levels. The data can be accessed immediately, and ground truthing field surveys can be timed to coincide precisely with the time

of flights. UAVs allow the collection of higher resolution imagery at a lower cost than manned aircraft or commercial satellite-data. UAV imagery resolution is typically less than 5cm per pixel, whereas manned aircraft resolution is typically 25-12.5 cm per pixel and satellite resolution is at best around 50 cm per pixel (Toth and Jozkow, 2016). Imagery acquired by the older generation of satellite sensors, at around 30 m per pixel, may pick up the dominant habitat but tend to lack the resolution required to represent the complex mosaics characteristic of many natural and semi-natural habitats (Boyle et al, 2014).

Image mosaic preparation, i.e. stitching the imagery together using off the shelf tools, remains a challenge due to the heterogeneity of habitats within landscape imagery, but is now automated in many software packages, and orthomosaics can be readily obtained. An important recent breakthrough is that a high resolution digital surface model (DSM) may also be obtained through Structure from Motion (SfM) photogrammetry processing in such software, since information on surface structure derived from the DSM may inform the relationship between subsequent classifications and peatland condition (Anderson et al. 2010). The combination of spectral data, DSM and classification techniques already available in the remote sensing scientist's toolbox (Random Forest Classification, maximum likelihood etc.) now provide huge potential to develop and calibrate an effective UAV-imagery based tool for peatland monitoring. Spectral and textural information have been combined successfully using Random Forest (a method based on machine learning that uses ensembles of decision trees to assign classes - see Breiman (2001) and Gislason et al. (2006)) for predicting forest condition (Dye et al. 2012), and for looking at fine scale coastal structures (Juel et al. 2015). Whilst uncertainties certainly exist in the use of SfM, uncertainties are simultaneously reduced if one considers how little detailed surface

topographic information exists for remote gully environments such as at Moor House NNR, used in this study.

In this paper we explore the potential of high spatial resolution (4 cm) true-colour (RGB) imagery obtained from a UAV platform for mapping and ecologically classifying a remote upland blanket bog in northern England. Since the surface topography of northern blanket bog habitats determine the presence of *Sphagnum*, *Eriophorum* or *Calluna* habitats, the models presented here incorporate a compound topographic index (CTI). Specifically we compared two input data scenarios and quantified the difference in the resulting classification:

Scenario 1: True-Colour orthomosaic only

Scenario 2: True-Colour orthomosaic, plus slope, CTI and aspect

We used two scenarios so that the effect that texture information might have on the accuracy of the peatland classification could be investigated. In particular we aimed to investigate the capability of the imagery to define small patches (< 1m width) of the fine scale habitats such as *Sphagnum* (a positive indicator of high water table), or exposed peat (negative indicator) that are poorly mapped by coarser resolution EO data. We considered how the information content of the input data could be maximised to improve classification accuracy. Finally we provide an estimate of carbon loss from an area of eroded peat based on: the elevation model, the classified eroded peat area, and the carbon density measurements taken through surveys at the site.

Methodology

Description of the study site

The UK Environmental Change Network (ECN) site, Moor House, Upper Teesdale, (OS Grid reference NY75303331), in the North Pennine uplands (Figure 1), is England's highest and

largest terrestrial National Nature Reserve (NNR). It is a UNESCO Biosphere Reserve and a European Special Protection Area. Habitats include exposed summits, extensive blanket peatlands, upland grasslands and pastures grazed mainly by sheep, hay meadows and deciduous woodland. A large part of the catchment of the River Tees, from its source near Great Dun Fell to High Force waterfall, is included in the reserve. The site comprises two areas divided by Cow Green Reservoir. The Moor House area extends from the upper edge of enclosed land in the Eden Valley, over Great Dun Fell (848 m), Little Dun Fell and Knock Fell to the upper end of Cow Green Reservoir on the River Tees. The gently sloping eastern side of the area is overlain by poorly-drained glacial till, which has led to the development of blanket bog with peat 2-3 m deep. The vegetation is dominated by *Eriophorum* spp., *Calluna vulgaris* and *Sphagnum* spp. with patches of eroded blanket bog without vegetation cover. The western side is steeper and the soils and vegetation are more variable. The area includes unique communities of arctic-alpine plants and upland flora and fauna of conservation interest.

Field Data Collection

A vegetation and landform survey was carried out between June and September 2008, and May and July 2009, as part of a wider objective to update habitat mapping within the Troutbeck catchment, a small catchment within the Moor House area (Rose et al., 2016). Quadrat sampling points were located systematically at the mid-points of a 100 m grid using ArcGIS (ESRI) (Figure 1), and located in the field using a handheld GPS unit (Garmin eTrex Vista HCx, accuracy < 3m).

Data were entered into a GIS database in the field using a modified version of the 'CS Surveyor' digital data capture system designed for Countryside Survey 2007 (Maskell et al. 2008). A 2 x 2 m^2 quadrat was placed at each plot, with the diagonal orientated north-south. Within each

quadrat, percentage cover of all vascular plant species, and a restricted list of bryophytes, was determined using visual estimation according to the technique described in Maskell et al. (2008).

Airborne Data Collection

The airborne campaigns were conducted in summer 2015 using an unmanned aerial vehicle (UAV) operated by the NERC Centre for Ecology and Hydrology. The UAV, a QuestUAV 300™, carried a Panasonic Lumix DMC-LX7 with a 3648 x 2736 pixel detector that captured JPEG images at f/1.4 and 1/2500s with an angular field of view of 73.7×53.1, providing ~4.5cm pixel^{-1} resolution at 122 m above ground level (AGL). The UAV was a 2 m wingspan fixed-wing platform with up to 1 h endurance at 3 kg take-off weight and 63 km/h ground speed. The UAV platform followed four flight plans over a 2400 m^2 area, which had been designed to ensure sharp imagery was obtained at high resolution, which had large across- and along-track overlapping. The UAV took 20 minutes to complete each flight plan at 122 m AGL. It was flown by two trained operators and controlled by an autopilot for fully autonomous flying (Skycircuits SC2, Southampton, UK). The autopilot had a dual CPU controlling an integrated attitude heading reference system (AHRS) with a comprehensive onboard sensor suite (3-axis accelerometers, 3-axis gyroscopes, 3-axis magnetometers, dynamic and static pressure sensors). The ground control station and the UAV were radio linked, transmitting position, altitude, and status data at 2.4 gHz. The weather on the date of the flights was clear and free of cloud. Flights were conducted between 10:00 and 16:00 to minimise effects of shadow. Wind speeds remained below 15 knots on all flights. The integrated onboard GPS updated at between 4 and 10 Hz and had a positional accuracy of +/-3 m.

Airborne Data Processing

The imagery was synchronized using the GPS position and the triggering time recorded on the flight logger for each image, and these were then used for the generation of an orthomosaic and digital surface model (DSM). Flight altitude data were also logged and images were geotagged with xyz coordinates for use by the image processing software. Image processing of the image collection was performed in Agisoft PhotoScan Professional v1.4.2 (© 2018 Agisoft LLC, 27 Gzhatskaya st., St. Petersburg, Russia). Details of the steps taken in acquisition, processing and modelling are shown in Figure 2. The software initially aligned the camera positions based on the GPS coordinates from the flight log. Ground control points were added based on known locations of static features located using 25cm Next Perspectives Aerial Photography RGB Product (Infoterra Ltd). Height values were based on values obtained from the Environment Agency LIDAR digital surface model which covered parts of the study area. Then a 3D point cloud, and 3D mesh representing the land surface was generated at a density of 160 points m^{-2}, this mesh was then used for orthomosaic and DSM generation at 0.04 m resolution. The Z error was computed by deducting check points Z values from the DSM value at the same point. The image processing settings and associated calculated accuracies are shown in Tables 4 and 5. During the stages of processing checks were made on image quality, tie point quality.

Topographic Processing

The DSM obtained from the image processing software was processed in ArcGIS 10.6 (ESRI, 2018). Slope, aspect, and a compound topographic index (CTI) (Sorensen et al., 2006) were generated at 4 cm resolution (see Figure 3) to be compatible with the RGB data. These figures show a subset of the data, and the gully features used for the Carbon loss estimation.

These data were then combined to yield a 6 band raster image containing red, green, blue, slope, aspect, and CTI values at 4 cm resolution.

Image Classification

The classification was trained on the 8 aggregate cover classes (Table 1) using all pixels within the digitised areas around each point. Specifically we compared two input data scenarios and quantified the difference in the resulting classification:

Scenario 1: Image Classification using Original RGB bands

The image obtained from the SfM procedures in Photoscan was processed using only the red, green and blue colourspace.

Scenario 2: Image Classification using Surface features and Original RGB Bands

The final image was processed using the red, green and blue colourspace, together with surface characteristics (gullies, edges) derived from the digital surface. The additional surface characteristics were added as separate bands to the image. These were slope, aspect, and CTI, all generated from the surface model at 4 cm resolution in ArcGIS 10.6 (ESRI, 2017).

The Random Forest (RF) classifier is an ensemble method that combines CART (Classification And Regression Trees) with bootstrap aggregating techniques (Breiman et al., 1984). Random Forests grow a number of binary classification trees by selecting a random sample with replacement from the training set (bootstrap aggregating or bagging) for each tree (Breiman, 1996). The predicted class for observations in the training set is the most frequent class in the trees for which the observation is a member. This process is described as "voting" (Breiman et al., 1984). The RF algorithm outputs the class label that received the majority of votes, and a probability estimate is derived for each pixel based upon the percentage of votes. The 6 band raster image, and companion training data for the 8 classes (Table 4) were supplied as inputs to

the algorithm, and the algorithm was processed in R (R Core Team 2015) using the Random Forest package by Liaw and M. Wiener (2002), and Horning (2013)

Field data Processing: Training data

The plant species cover data from the quadrats were automatically assigned to the nearest National Vegetation Classification (NVC), (Rodwell, 1995.) sub-community using the MAVIS program (Smart, 2000) which uses Czekanowski's quantitative index of similarity, taking into account the abundance as well as presence of species (Magurran, 1998). This supervised classification of the data was then visually checked against photographs taken at the date of sampling. If there were discrepancies the assigned class was corrected according to a visual interpretation from the photography. The areas were manually digitised in GIS in order to encapsulate the habitats of a similar type around the plot, so that for a 10 m diameter zone around each plot, the dominant habitat type was described, and the other habitat areas removed, leaving just the habitat of interest for each plot. For example *Sphagnum* areas only were digitised, for a plot classed as *sphagnum*. These vegetation classes were aggregated according to one of 8 types (Table 1) for ease of classification. In addition, 20 ground control points were identified from Environment Agency Lidar 2m DSM (Environment Agency © 2015) at fixed locations identified using 25cm Aerial imagery (Infoterra, © 2014).

Field data processing: Validation data

Validation points were randomly stratified across the 8 classes in ArcGIS 10.8 (ESRI, 2016), with 10 points within each class. These points were then used to sample the classifications and assess the performance of the random forest classification.

Evaluation and validation

To assess the accuracy of an image classification, a confusion matrix was created which compared the classification results with the validation data. This identifies the nature of the classification errors, as well as their quantities. Confusion matrices were produced from the overlay of the validation areas and the resultant spatial classification. Overall Accuracy (OA) values were computed from confusion matrices in order to evaluate the accuracy of the produced land cover maps (Congalton, 1991). User and producer accuracy was also calculated. Producer accuracy is the fraction of correctly classified pixels with regard to all pixels of that ground truth class, whereas user accuracy (or reliability) is the fraction of correctly classified pixels with regard to all pixels classified as this class in the classified image. A kappa statistic (Cohen, 1960), that compares the accuracy of the system to the accuracy of a random system, was computed against the validation data. Probability estimates derived from the model (the percentage votes for each pixel) were grouped by class, and the mean taken for each group to assess the quality of the predictions.

Carbon loss Estimation

The area surveyed at Moor House contains a number of erosion features and gullies. One gully is of considerable size, and an estimate of the net loss of carbon through the peat degradation and erosion is of interest. From previous studies of the site, a measurement of the eroding gully carbon density is 69.84 ± 2.74 mg C cm^3 (Whitfield 2012). The area of the gully was first covered with a hypothetical surface (assumed flat) at 4 cm spatial resolution, to cover the edges of the gully, and only where bare peat was exposed. This follows the method of Evans and Lindsay (2010), who used linear interpolation of the DEM between gully edges defined from the gully map to create a 'pre-erosion' surface; and then subtracted the contemporary surface from the pre-erosion surface to create a gully depth map. Using a cut – fill model in QGIS (QGIS

Development Team, 2017), a hypsometric model of the eroded gully was then created. Using this estimate of volume and the carbon density measurements for the Moor House site allowed an estimate of the carbon loss to be calculated.

Results

The SfM derived imagery yielded a 4 cm resolution orthomosaic (Figure 1). The elevation model obtained from the image processing was used to compute the aspect, slope and topographic index maps shown in Figures 3. The classifications computed by the RF classifier yielded the classification maps and probability estimates in Figures 4 to 7.

Confusion matrices were produced to assess the accuracy of the classified image using both data input scenarios (Table 2 and 3). These matrices show the accuracy of the predictions for the external validation areas, which are independent of the training areas used for establishment of the classification models. For scenario 1, using RGB data only, the classification accuracy per class varied between 40 and 100%. The highest classification accuracy in this case was for coniferous woodland, with the lowest being for bare peat. The overall kappa coefficient was 0.66 (Table 2). For scenario 2, using RGB and surface topography data, the classification accuracy per class varied between 50 and 100%. The highest classification accuracy was for conifer plantation, and the lowest was for bare peat. The overall kappa coefficient was slightly higher at 0.68 (Table 3).

Mean probability values for each classification are shown in Figure 7 and ranged from 41% (Saturated bog) to 67% (coniferous woodland). For all classes, the mean classification probability was higher for the RGB plus topography classification.

Carbon loss estimate

The volume of material lost in the formation of the gully, assuming an intact blanket bog formation prior to erosion, was estimated as 6,273 m^3. The carbon density for gullies at Moor House is 69.84 ± 2.74 mg C cm^3. Therefore the estimated carbon that has been lost from the gully is estimated to be between 420 and 455 tonnes of C.

Discussion

The results of the image classification using a Random Forest classifier are encouraging, and demonstrate the potential for rapid reconnaissance and monitoring of blanket bog condition (*per se*) nationally. Incorporation of surface feature data derived from SfM techniques improved the classification accuracy. The incorporation of surface data improves the classification by defining those areas where water accumulates in the landscape, thereby assisting the classification of the smaller *Sphagnum* bog areas. Incorporation of surface topography improved the predictive accuracy, in part due the presence of specific habitats in dry or wet areas of the blanket bog. For example *Sphagnum* carpet is only ever found in specifically wet channels or funnels at the Moor House site. Conversely, exposed bare peat may only be found on the flat tops or edges of the blanket bog (Bower, 1961), where water accumulates, and hard frost and wind can attack the structure of the peat. The centre of the blanket bog is characterised by a large eroding mass of peat. This is not surprising since peat erosion is associated with high levels of exposure and precipitation (Bragg, 2001;Yeloff et al. 2005). The Random Forest classifier accurately predicted all classes specified in the training data. Interestingly, although the classification accuracy (user accuracy) for bare peat was 50%, saturated bog, water and sphagnum were higher, ranging between 80% and 90%. Saturated bog, water and bare peat habitats are often in very close proximity in the study area, and only by using aerial photography at 4cm resolution could we

locate habitat patches at such fine a scale. Future studies could look at how much bare peat exists elsewhere in the study area, in addition to the central exposed peat area.

The probability of the classification is slightly higher for all classes when topography is used in addition to the RGB data. This may in part be due to high spatial variability in the surface topography exceeding that encompassed within the training data. Also, the incorporation of more predictor variables in Random Forests may yield greater certainty, as a result of the model structure. The mean probability estimates are acceptable (i.e. generally above the default value of 0.5), however it is worth noting that Random Forest classifiers normally give good estimates (Belgiu and Dragut 2016), probably due to the transitional nature of upland habitats. Further studies should explore the effect of sample data collection and survey date on the classification. In some cases an accurate Random Forests model can give poor probability estimates (Yang et al. 2016), so the percentage of correctly classified test data is the most common criterion to evaluate models (Bostrom 2007). Therefore comparison of both scenarios accuracies based on mean probabilities could be misleading.

Although the vegetation survey data and the aerial survey were six years apart, the use of site photography taken on the date of the vegetation survey (2010) allowed a comparison of the present situation with the state of the land surface in 2014 to be accomplished, and showed that vegetation composition was not significantly different. We cross referenced photographs from the study site taken at the time of the botanical survey, with 25 cm resolution aerial photography, and our own orthorectified imagery to ensure that the training areas had not changed significantly, thus minimising any uncertainty associated with the classification of training areas.

Ideally, vegetation surveys should be undertaken at least during the same year of the aerial survey to reduce this uncertainty.

As with all modelling and data collection methodologies there are uncertainties arising from the various stages of data acquisition, and implicit uncertainties in the modelling, either as a result of the data or the structure of the modelling framework. The uncertainties in the data may arise through the temporal mismatch between the date of image acquisition and the land survey, and this may explain some of the misclassification of water as peat and vice versa.

The purpose of this study was to investigate the area of blanket peatland under erosion, and quantify the apparent losses. This was achieved with some success, but also some uncertainty, since the volume of intact blanket peatland prior to the formation of gully and erosion features can never be fully known. The true volume of carbon that has been lost cannot be calculated, since the bog would have gradually lost and simultaneously sequestered carbon through revegetation and recovery over time. Also, the hypothetical surface used to calculate the volume could be Estimating a value is, however, useful in providing the conservation scientist with a value associated with the formation of gully features, and what could potentially be recovered through habitat restoration.

The methodology, combining ground- and UAV-based survey, and ground control points based on static objects, is readily transferable to other sites containing different habitats. When combined with topographic indices, slope and aspect, RGB data can be extremely useful in remote areas where habitat classification can be difficult due to limited access or data availability. Although ground control points should normally be located using a high accuracy GPS unit, such systems were unavailable to the team at the time, and the purpose of this study was to minimise impact at the site, especially in the upland saturated bog environment. Future studies could however make use of onboard RTK systems for improved camera location accuracy, and improved ground control point accuracy for the static locations. While

hyperspectral data from UAVs are still expensive to obtain, the approach provided here can provide equivalent outputs with a similar level of accuracy. UAVs may therefore fill the gap between land surveys and satellite imagery. UAVs do have some drawbacks compared to more traditional sources of remote sensing data. Specifically, UAVs are more limited in their sensor payload, and therefore the complexity of sensors that they can carry, although this is due to a combination of cost, ease of use and regulations. UAVs are also more susceptible to high winds and adverse weather compared to manned aircraft. Wind speeds above 15 knots (35 mph) typically lead to poor image capture from a UAV. Individual flights cover much smaller areas compared to manned aircraft and satellites. Therefore more flights are required to cover larger areas and more time is required to process the imagery produced. Larger areas (multiple km^2) could be captured per flight using fixed wing UAVs, however this approach is limited by visual flight rule requirements. RGB data from UAV platforms can also fill the gap between field and satellite imagery, which are either labour intensive or conversely too coarse resolution to separate distinct habitats within the broad habitats. UAV hyperspectral data are still prohibitively expensive, so the combination of UAV RGB data with topography data can be useful for upland habitats in the UK where the access is difficult and availability of satellite imagery is low due to cloud coverage.

Conclusions

There is a greater availability of UAV platforms providing RGB imagery at present, owing in part to the expense of hyperspectral instruments. This study demonstrates that for large areas of fairly homogenous and well defined habitats, habitat classifications may be produced in a relatively cheap and easy way using consumer grade cameras and relatively inexpensive fixed wing UAV platforms. Remote sensing of upland sites in the UK can be difficult due to cloud

cover, and therefore UAVs may offer an effective and realistic alternative. Combined with open source software approaches for image classification, this approach presents new opportunities for directing, and monitoring the success of peatland conservation schemes. As a specific means of measuring success, carbon loss estimates can be readily generated using the UAV imagery and SfM techniques described here.

Acknowledgments

We thank the NERC Centre for Ecology and Hydrology for providing the internal funding for the purposes of this work.

References

Anderson, K., Bennie, J.J., Milton, E.J., Hughes, P.D.M., Lindsay, R., & Meade, R. (2010) Combining LiDAR and IKONOS Data for Eco-Hydrological Classification of an Ombrotrophic Peatland. *Journal of Environmental Quality*, 39, 260-273

Anderson, K. and Gaston, K. J. (2013) Lightweight unmanned aerial vehicles will revolutionize spatial ecology. *Frontiers in Ecology and the Environment*, 11: 138–146. doi:10.1890/120150

Belgiu, M., & Dragut, L. (2016). Random forest in remote sensing: A review of applications and future directions. *Isprs Journal of Photogrammetry and Remote Sensing*, 114, 24-31

Bostrom, H. (2007) Estimating class probabilities in random forests. In Machine Learning and Applications, 2007. ICMLA 2007. Sixth International Conference on, pp. 211-216. IEEE, 2007.

Boyle S.A., Kennedy C.M., Torres J., Colman K, Pérez-Estigarribia P.E., de la Sancha N.U. (2014). High-Resolution Satellite Imagery Is an Important yet Underutilized Resource in Conservation Biology. Peter H-U, ed. *PLoS ONE*., 9(1):e86908. doi:10.1371/journal.pone.0086908.

Bower M, (1961). The distribution of erosion in blanket peat bogs in the Pennines. *Transactions of the Institute of British Geographers*, 29: 17-30

Bragg, O M & J H Tallis, (2001) The sensitivity of peat-covered upland landscapes. *Catena*, 42: 345-360.

Breiman L. (2001) Random Forests. Machine Learning, 45, 5–32.

Breiman, L., Friedman, J. H., Olshen, R. A., & Stone, C. J. (1984) Classification and regression trees. Monterey, CA: Wadsworth & Brooks/Cole Advanced Books & Software. Breiman, L. 1996. Bagging Predictors. Machine Learning 24:123-140.

Cohen, J. (1960) A coefficient of agreement for nominal scales. *Educational and Psychological Measurement* 20, 37-46.

Congalton RG. (1991) A Review of Assessing the Accuracy of Classifications of Remotely Sensed Data. *Remote Sensing of Environment* 37: 35-46.

Dye, M., Mutanga, O., & Ismail, R. (2012) Combining spectral and textural remote sensing variables using random forests: predicting the age of Pinus patula forests in KwaZulu-Natal, South Africa. *Journal of Spatial Science*, 57, 193-211

Environmental Systems Research Institute (ESRI) (2010). ArcGIS Release 10. Redlands, CA.

Evans, C.D., Bonn, A., Holden, J., Reed, M.S., Evans, M.G., Worrall, F., Couwenberg, J., & Parnell, M. (2014) Relationships between anthropogenic pressures and ecosystem functions in UK blanket bogs: Linking process understanding to ecosystem service valuation. *Ecosystem Services*, 9, 5-19

Evans, M. and Lindsay, J. (2010) High resolution quantification of gully erosion in upland peatlands at the landscape scale. *Earth Surface Processes and Landforms*, 35: 876–886. doi:10.1002/esp.1918

Freeman, C., Evans, C.D., Monteith, D.T., Reynolds, B., & Fenner, N. (2001) Export of organic carbon from peat soils. *Nature*, 412, 785-785

Gislason P.O., Benediktsson J.A., & Sveinsson J.R. (2006) Random Forests for land cover classification. Pattern Recognition Letters, 27, 294–300.

Glendell, M., McShane, G., Farrow, L., James, M. R., Quinton, J., Anderson, K., Evans, M., Benaud, P., Rawlins, B., Morgan, D., Jones, L., Kirkham, M., DeBell, L., Quine, T. A., Lark, M., Rickson, J., and Brazier, R. E. (2017) Testing the utility of structure-from-motion photogrammetry reconstructions using small unmanned aerial vehicles and ground photography to estimate the extent of upland soil erosion. *Earth Surface Processes and Landforms*, 42: 1860–1871. doi: 10.1002/esp.4142.

Gorham, E. (1991) Northern peatlands: role in the carbon cycle and probable responses to climatic warming. *Ecological Applications*, 1: 182-195

Holden J. (2005) Peatland hydrology and carbon release: why small-scale process matters. *Philosophical Transactions of the Royal Society a-Mathematical Physical and Engineering Sciences* 363: 2891-2913.

Horning, N. (2013) Training Guide for Using Random Forests to Classify Satellite Images – v9. American Museum of Natural History, Center for Biodiversity and Conservation. Available from http://biodiversityinformatics.amnh.org/. https://doi.org/10.5285/7a7d08e3-48e2-4aad-855b-9d6767b9ae9b

Joosten H., Tapio-Biström M.-L. & Tol S. (eds) (2012) Peatlands –guidance for climate change mitigation through conservation, rehabilitation and sustainable use. 2nd ed. FAO and Wetlands International, Rome, Italy, 100 pp. ISBN: 978-92-5-107302-5

Juel, A., Groom, G.B., Svenning, J.C., & Ejrnaes, R. (2015) Spatial application of Random Forest models for fine-scale coastal vegetation classification using object based analysis of aerial orthophoto and DEM data. *International Journal of Applied Earth Observation and Geoinformation*, 42, 106-114

Liaw and M. Wiener (2002). Classification and Regression by randomForest. R News 2(3), 18--22.

Littlewood, N., Anderson, P., Artz, R., Bragg, O., Lunt, P. and Marrs, R. (2010) Peatland biodiversity. Report to IUCN UK Peatland Programme, Edinburgh. www.iucn-uk-peatlandprogramme.org/scientificreviews

Magurran, A.E. (1988) Ecological diversity and its measurement. London: Croon Helm Ltd. 179 p.

Maskell, L.C., Norton, L.R., Smart, S.M., Carey, P.D., Murphy, J., Chamberlain, P.M., Wood, C.M., Bunce, R.G.H. & Barr, C.J. (2008) *Countryside Survey Technical Report No. 1/07 Field Mapping Handbook*.
http://www.countrysidesurvey.org.uk/sites/default/files/pdfs/reports2007/CS_UK_2007_TR1.pdf

Mc Morrow, I.M., Cutler, M.E., Evans, M, Alroichdi, A., (2004), hyperspectral indices for characterising upland peat composition. *International journal of remote sensing*, 25, 313-325.

R Core Team (2013). R: A language and environment for statistical computing. R Foundation for Statistical Computing, Vienna, Austria. URL http://www.R-project.org/.

QGIS Development Team (2017). QGIS Geographic Information System. Open Source Geospatial Foundation Project. http://qgis.osgeo.org

Rodwell, J.S. (ed.) (1995). *British Plant Communities. Volume 4.* Aquatic communities, swamps and tall-herb fens. Cambridge University Press.

Rose, R.J., Wood, C.M., Baxendale, C.L., Whitfield, M.G., Ostle, N.J., Driscoll, B., Looker, A., Looker, G. (2016). Vegetation survey of Moor House National Nature Reserve 2008-2009.

NERC Environmental Information Data Centre https://doi.org/10.5285/7a7d08e3-48e2-4aad-855b-9d6767b9ae9b

Smart, S.M. (2000) MAVIS: Modular Analysis of Vegetation Information System.: Centre for Ecology and Hydrology, Lancaster, UK. Available: http://www.ceh.ac.uk/services/modular-analysis-vegetationinformation-system-mavis.

Sørensen, R.; Zinko, U.; Seibert, J. (2006) "On the calculation of the topographic wetness index: evaluation of different methods based on field observations". *Hydrology and Earth System Sciences*. 10: 101–112.

Toth C and Jozkow G. (2016) Remote sensing platforms and sensors: A survey. *Isprs Journal of Photogrammetry and Remote Sensing* 115: 22-36.

Whitfield, M.G. Peatland diversity and carbon dynamics, Thesis submitted for the degree of Doctor of Philosophy, Lancaster University, September 2012.

Yang, F., Piao P., and Qifeng, Z. (2016) A preliminary study on class probability estimation for random forest using kernel density estimators. *Computer Science & Education (ICCSE)*, 2016 11th International Conference on. IEEE, 2016.

Yeloff, D.E., Labadz, J.C., Hunt, C.O., Higgitt, D.L., & Foster, I.D.L. (2005) Blanket peat erosion and sediment yield in an upland reservoir catchment in the southern Pennines, UK. *Earth Surface Processes and Landforms*, 30, 717-733

Yu ZC. (2012) Northern peatland carbon stocks and dynamics: a review. *Biogeosciences* 9:4071-4085.

457

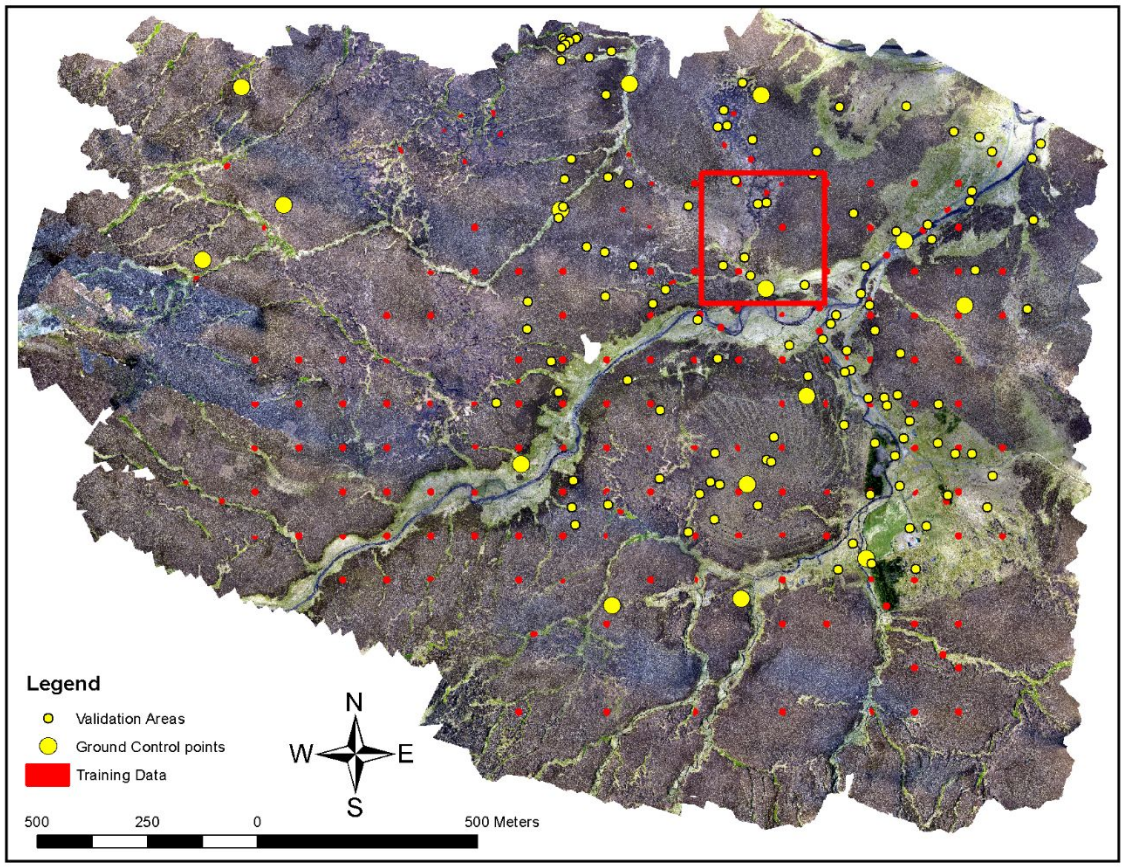

Figure 1 Overview of the Troutbeck study area at Moor House ECN, showing the orthorectified image obtained from 4 UAV flights, ground control points, the model training and validation areas and the focus area (red square).

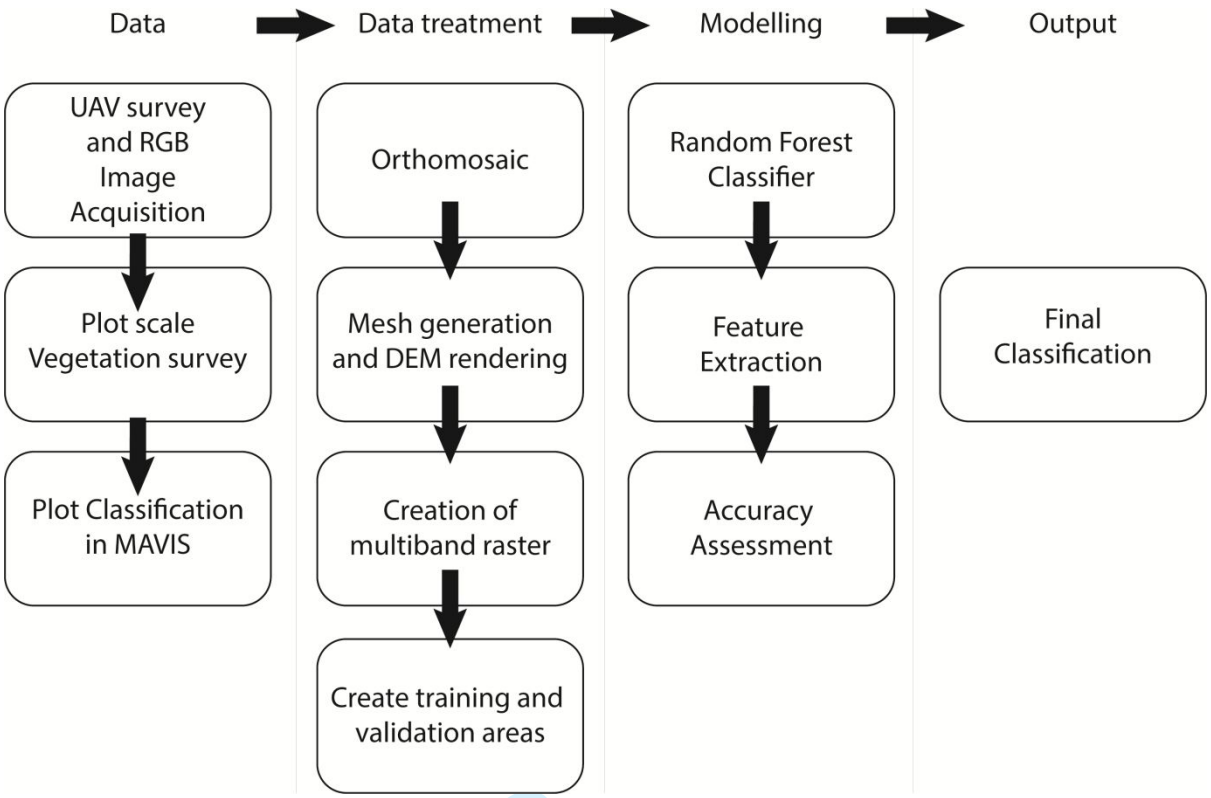

Figure 2 Process flow from image capture to the final habitat classification used in this study.

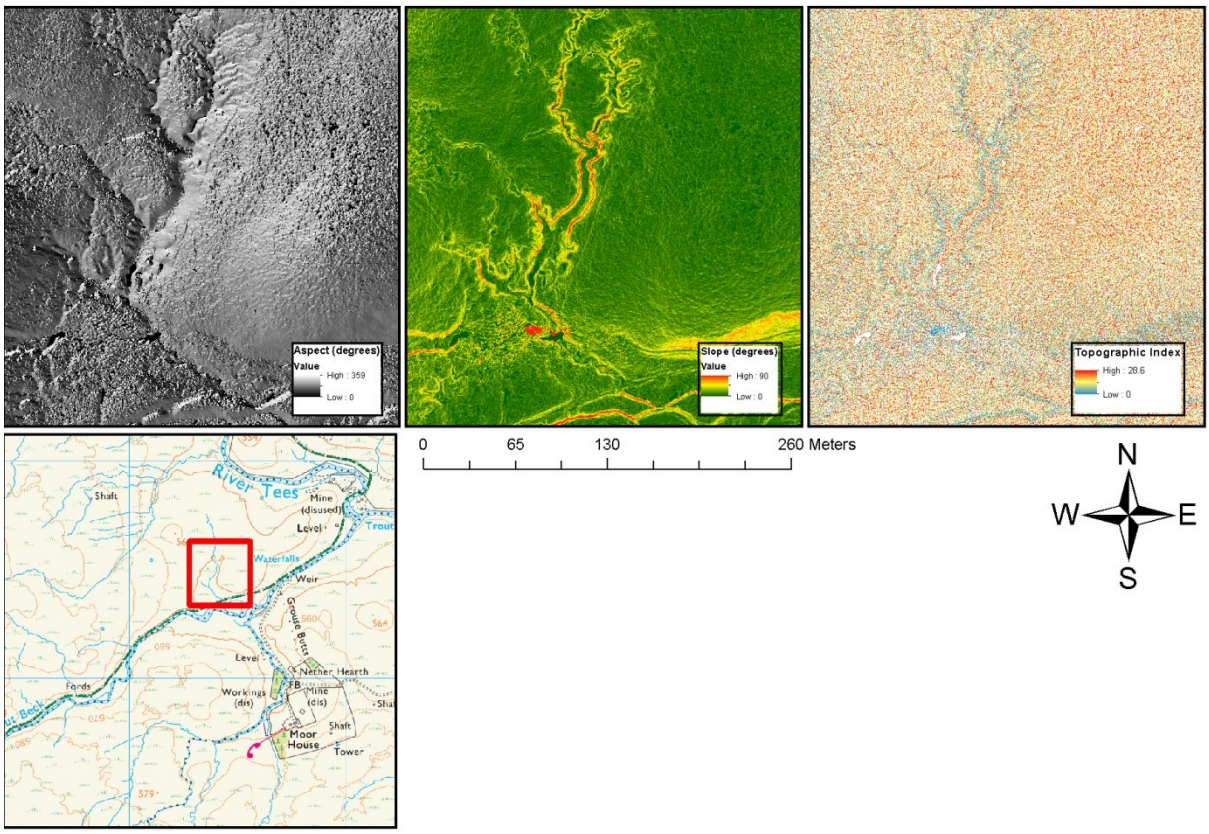

Figure 3 Aspect, slope and topographic index surfaces generated from the surface topography (4 cm spatial resolution). Area of the eroded gully shown, maps extend across the whole Moorhouse study area.

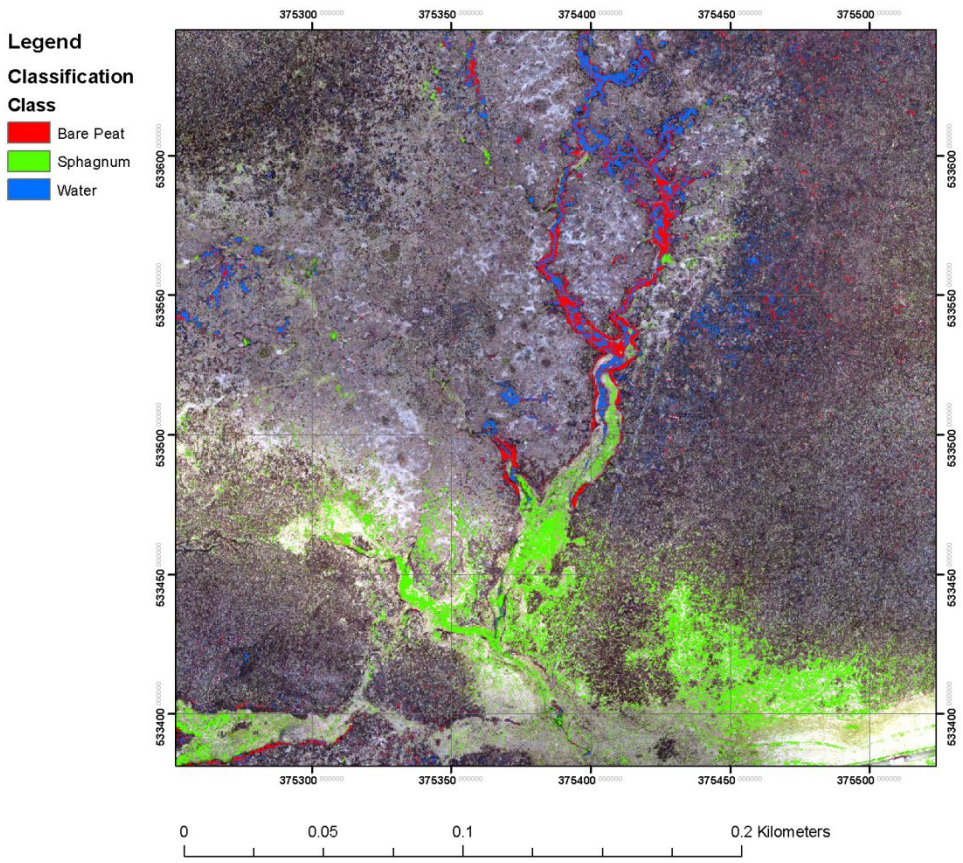

Figure 6 Map showing the bare peat, water and sphagnum habitats as predicted for Moor House with RGB and topographic information for the focus area.

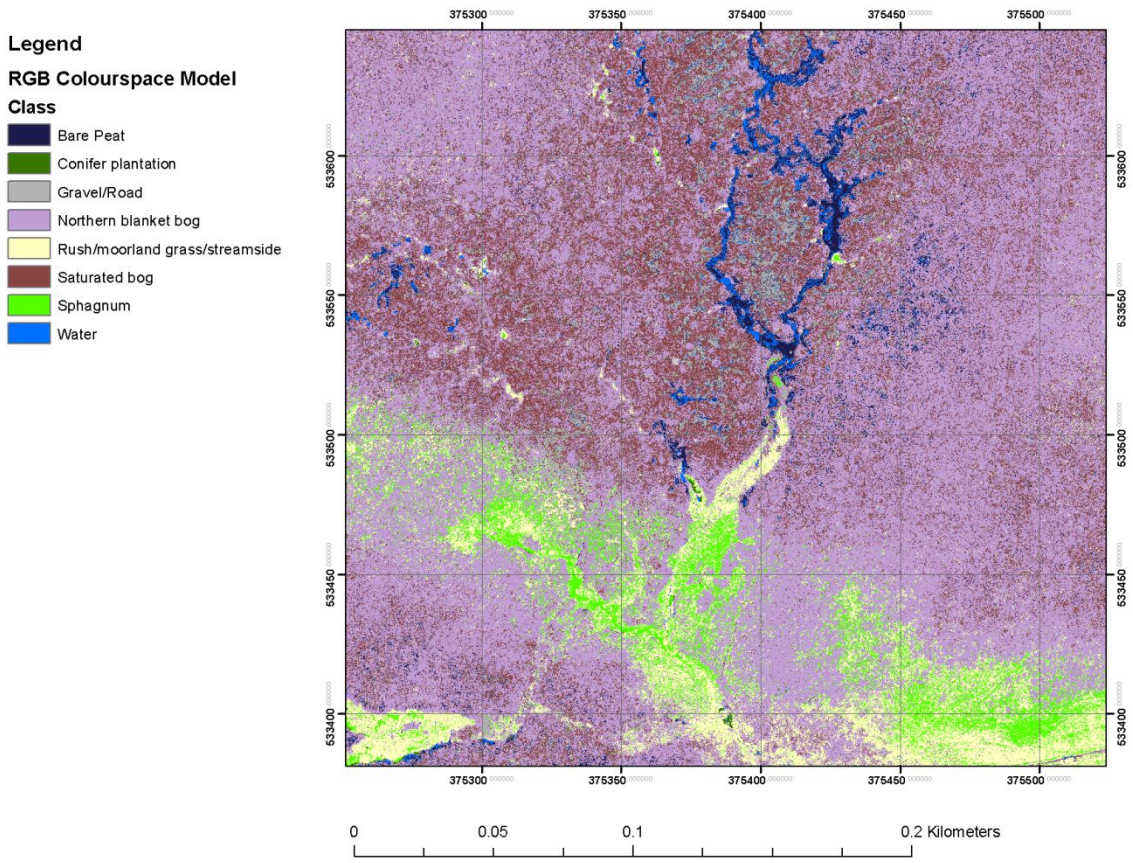

Figure 7 Predicted classes for Moor House using only the RGB data

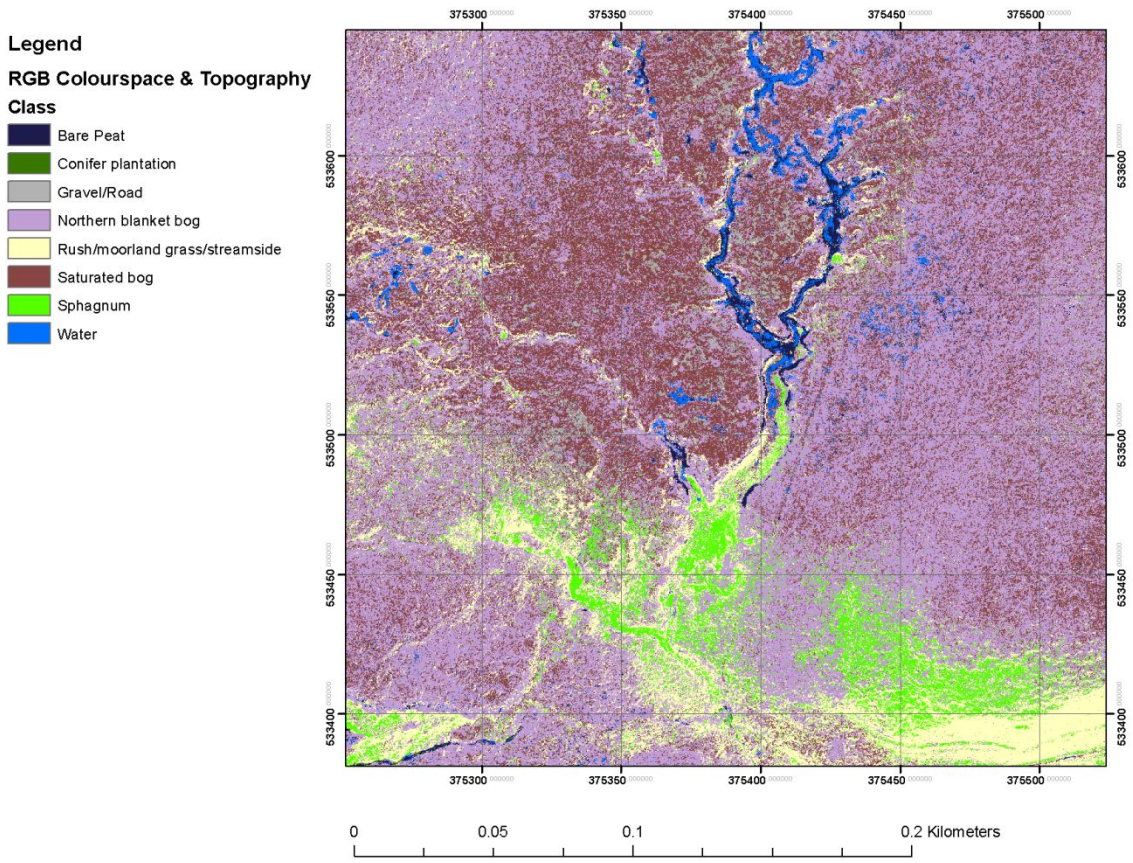

Figure 8 Predicted classes for Moor House using the RGB combined with the topographic information

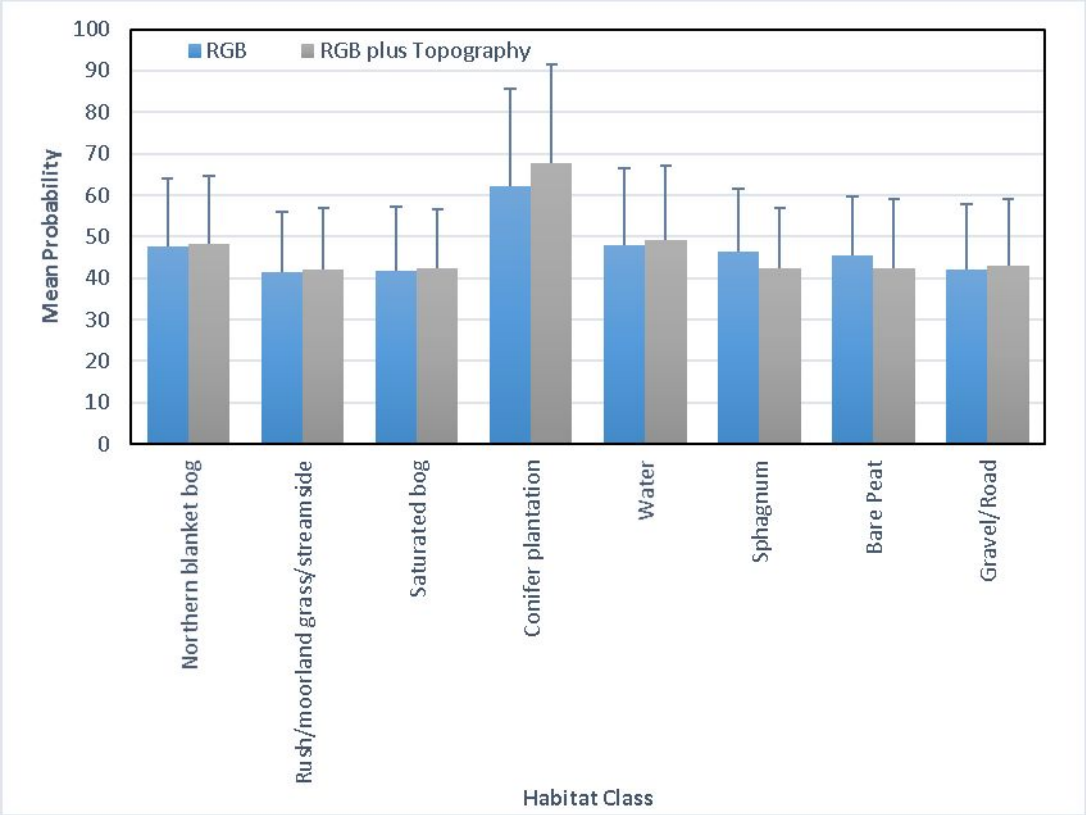

Figure 9 Mean probabilities for each surface summarised for each classification with standard errors.

Table 1 List of aggregated classes based on the Countryside Vegetation System used in this study

CVS Class	**Aggregate Class**
Northern Blanket Bog	Northern Blanket Bog
Dry heath soil	Bare Peat
Bare Peat	
Young conifer	Conifer plantation
Conifer plantation	
River shingle	Gravel
Streamside/acid grassland	Moorland Grass
Bracken/acid grass	
Moorland grass/bog	
Moorland grass/heath peat	
Marsh/streamside	
Moorland grass/heath soil	
Heath/moorland grass	
Saturated bog	Saturated bog
Sphagnum	Sphagnum
Open Water	Open Water

Table 2 Confusion Matrix for the random forest classification using only the RGB data for Moor House

		Predicted									
		Northern blanket bog	Rush/moorland grass/streamside	Saturated bog	Conifer plantation	Water	Sphagnum	Bare Peat	Gravel/Road	Total	User accuracy (%)
Actual	Northern blanket bog	8	0	2	0	0	0	0	0	10	80
	Rush/moorland grass/streamside	0	10	0	0	0	0	0	0	10	100
	Saturated bog	2	1	7	0	0	0	0	0	10	70
	Conifer plantation	0	0	0	9	1	0	0	0	10	90
	Water	0	0	2	0	7	0	0	1	10	70
	Sphagnum	0	1	0	0	0	9	0	0	10	90
	Bare Peat	3	0	1	0	2	0	4	0	10	40
	Gravel/Road	1	0	2	0	0	0	0	7	10	70
	Total	14	12	14	9	10	9	4	8		
	Producer accuracy (%)	42	83	50	100	70	100	100	88		
	Kappa	0.68									

Table 3 Confusion Matrix for the random forest classification using the RGB data and surface topography for Moor House

		Predicted									
		Northern blanket bog	Rush/moorland grass/streamside	Saturated bog	Conifer plantation	Water	Sphagnum	Bare Peat	Gravel/Road	Total	User accuracy (%)
Actual	Northern blanket bog	9	0	1	0	0	0	0	0	10	90
	Rush/moorland grass/streamside	1	9	0	0	0	0	0	0	10	90
	Saturated bog	1	0	8	0	1	0	0	0	10	80
	Conifer plantation	0	0	0	10	0	0	0	0	10	100
	Water	1	0	0	1	8	0	0	0	10	80
	Sphagnum	0	1	0	0	0	9	0	0	10	90
	Bare Peat	1	1	1	0	2	0	5	0	10	50
	Gravel/Road	0	2	1	0	0	1	0	6	10	60
	Total	13	14	11	11	11	10	5	6		
	Producer accuracy (%)	41	64	73	91	73	90	100	100		
	Kappa	0.66									

Table 1 Processing parameters used in Agisoft Photocsan for the construction of the orthomosaic and digital surface model

General	Cameras 2207 Aligned cameras 2207 Markers 24 Coordinate system OSGB 1936 / British National Grid (EPSG::27700) Rotation angles Yaw, Pitch, Roll
Point Cloud	Points 440,842 of 638,731 Reprojection error 1.2099 (7.04299 max) Point colors 3 bands, uint8 Key points No Average tie point multiplicity 3.75116
Dense Point Cloud	 Points 625,020,795 Point colors 3 bands, uint8
Dense Point Cloud Reconstruction parameters	Quality High Depth filtering Aggressive
Model	Faces 4,925,688 Vertices 2,473,776 Vertex colors 3 bands, uint8 Texture 4,096 x 4,096, 4 bands, uint8
Model Reconstruction parameters	Surface type Height field Source data Dense Interpolation Enabled Quality High Depth filtering Aggressive Face count 5,000,000 Processing time 20 minutes 12 seconds
Model Texturing parameters	Mapping mode Orthophoto Blending mode Mosaic Texture size 4,096 x 4,096 Enable hole filling Yes Enable ghosting filter Yes UV mapping time 1 minutes 37 seconds Blending time 9 hours 46 minutes
DSM	Size 52,504 x 46,139 Coordinate system OSGB 1936 / British National Grid (EPSG::27700)
DSM Reconstruction parameters	Source data Dense cloud Interpolation Enabled Processing time 55 minutes 24 seconds
Orthomosaic	Size 65,494 x 52,584 Coordinate system OSGB 1936 / British National Grid (EPSG::27700) Colors 3 bands, uint8
Orthomosaic Reconstruction parameters	Blending mode Mosaic Surface DEM Enable hole filling Yes Processing time 1 hours 15 minutes

Table 5. Control points RMSE and ground control point (GCP) errors , (X - Easting, Y - Northing, Z – Altitude).

Point type	**Count**	**X error (m)**	**Y error (m)**	**Z error (m)**	**XY error (m)**	**Total (m)**
Control	15	1.75774	0.485608	1.43344	1.82359	2.31953
	Label	**X error (m)**	**Y error (m)**	**Z error (m)**	**Total (m)**	**Image (pix)**
	Bridge	-0.469988	-0.100511	-0.728492	0.87275	0.000 (1)
	point 1					
	point 2	-0.499273	0.0301792	0.249121	0.55879	0.000 (1)
	point 3	-0.936561	-0.487554	-1.5222	1.85256	0.002 (4)
	point 4	2.05486	-0.616093	-3.03196	3.71413	0.002 (2)
	point 5					
	point 6	0.0944338	0.510288	0.282165	0.590702	0.000 (1)
	point 7					
	point 8	0.220504	-0.0945066	1.2857	1.30789	0.005 (7)
	point 9	0.261059	-0.448917	2.29679	2.35477	0.003 (3)
	point 10	-0.106125	-0.870693	-1.06144	1.37696	0.005 (3)
GCP	point 11	0.384385	-0.632363	0.320792	0.806562	0.001 (3)
	point 12	0.659767	0.174325	-1.05869	1.25956	0.003 (4)
	point 13					
	point 14					
	point 15					
	point 16	-6.03509	-0.503942	-1.11076	6.15711	0.002 (3)
	point 17					
	point 18					
	point 19	1.41136	-0.343287	1.09074	1.81645	0.003 (3)
	point 20	0.972456	0.651922	1.50597	1.90752	0.003 (3)
	point 21	0.823755	0.0132818	2.07568	2.2332	0.002 (3)
	point 22					
	point 23	-0.128602	0.67285	-0.600468	0.910949	0.002 (2)